Indian Journal of Science and Technology, *Vol 8(17), DOI: 10.17485/ijst/2015/v8i17/65958, August 2015*

ISSN (Print) : 0974-6846
ISSN (Online) : 0974-5645

Buckling Analysis of Bimodular Laminated Plates: A Comparative Study using New Modified Higher Order Theory

Masoud Kazemi*

Faculty of Engineering, Department of Mechanics, Islamshahr Branch, Islamic Azad University, Islamshahr, 67653-33147, Iran; kazemii@iiau.ac.ir, masoud_kazemi@hotmail.com

Abstract

Elastic instability (buckling) results for a bimodular laminated plate based on a modified higher order plate theory with seven kinematic variables are presented. Buckling coefficients obtained by the present theory are compared with the Mindlin plate theory (first order plate theory) results higher order plate theory results. A detailed parametric study is carried out to investigate the influence of bi-modularity, thickness ratio, aspect ratio and lamination scheme on the critical buckling load response. The present modified higher order plate theory satisfies the stress-free boundary conditions and predicts buckling loads very accurately. Also, the benefit of significant simplification can be observed as compared with the Lo et al. higher order plate theory.

Keywords: Bimodular, Buckling, Composite, Laminates

1. Introduction

Laminated fibrous composite plates are extensively being used in different industries such as aerospace, aircraft, automobile and audio industries to fabricate structures with high performance. They are attractive replacements for conventional metal plates, but their analysis and design are more complex than isotropic metal plates due to material anisotropy[1].

The modern theory of elasticity assumes that the strain (deformation) of an elastic material is proportional to the stress applied to it. Generally the elastic moduli that connect stress and strain rely on the orientation of the coordinate axes. Many researchers have demonstrated that some materials, behave differently in tension and compression. These include for example, tyre cord-rubber materials, ceramics, graphite, and some composites[2]. These kinds of materials are called bimodulus, bi-modular, bilinear or different-modulus materials[3]. Because of non-linearity behavior of these materials, a bilinear model is required as an approximate method of representing the moduli. Studies of the behavior of bimodular materials are of practical importance as a result of increasing use of these materials in structures.

It is necessary to develop a model to predict the response of bimodular composites, but the analysis of bimodular materials is more complicated than ordinary materials since the elastic modulus depend on the signs of the stresses.

The concept of a bimodular structure was introduced by Timoshenko[4]. The basic material model describing the behavior of bimodular materials was introduced by Ambartsumyan and Khachatryan[5]. The bending of bimodular material plates has been studied in some published researches; Shapiro[6] considered the very simple problem of a circular plate subjected to a pure radial bending moment at its edge. Kamiya[7] used a numerical analysis for a high-polymer circular shell subjected to a uniform internal pressure. Results showed that the distribution of axial and circumferential bending moments in the circular shell varies with the difference between the tensile and compressive moduli of elasticity. Also, Kamiya[8] treated large deflections of a different-modulus elastic plate subjected to a uniform lateral load by the finite difference method. Kamiya also applied the energy method to the large deflection analysis of a

* *Author for correspondence*

rectangular bimodular plate based on thin plate theory[9]. More recently, Sun et al.[10] reviewed mechanical problems with different moduli in tension and compression.

The results suggested that researches should be concentrate to the laminates with a large E^t/E^c ratio. A macroscopic model analysis of bimodular fiber-reinforced composites made by Bert[11] and the results agree with experimental tests. Bert[12] used the macroscopic material model to study bimodular composite laminated plates using the finite element method. Also, Bert et al. extended this work to the vibrational analysis of thick rectangular plates[13] and cylindrical shells[11] of bimodular composite materials. The finite element analysis of bimodular laminated plates by Reddy et al.[14] uses a displacement finite element method and Bert et al.[15] use a mixed finite element method, in the context of Mindlin plate theory.

Few works of the buckling problem of bimodular laminates have been published in the literature. Jones[16,17] investigated the buckling of circular cylindrical shells and stiffened multilayered circular cylindrical shells on the basis of the Ambartsumyan model[5]. Bert and Reddy[18] used a closed form and finite element method to study the vibration and buckling of thick shells of bimodular composite materials. The buckling load is found by determining the lowest axial compressive load for which the natural frequency is also the lowest.

Hajmohammad et al.[19] used Genetic algorithm approaches for the optimal design of composite laminates subjected to the axial compression loading. All subjects related to the anisotropic elastic plates are collected from published results have been rewritten using a unified notation by HWU[20].

Reissner[21] and Mindlin[22] presented generalizations of classical plate theory incorporating transverse shear deformation by using a transverse shear correction factor. The incremental displacements are assumed to be of the following form:

$$\begin{aligned}\bar{u}_1(x,y,z,t) &= u_x(x,y,t) + z\varphi_x(x,y,t)\\ \bar{u}_2(x,y,z,t) &= u_y(x,y,t) + z\varphi_x(x,y,t)\\ \bar{u}_3(x,y,z,t) &= w(x,y,t)\end{aligned} \tag{1}$$

where z is the coordinate normal to the middle plane $u'_x u'_y$ and ω are displacements of the neutral surface. φ_x and φ_y account for the effect of transverse shear. Despite the increased generality of the above theory the related flexural stress distributions show only little advancement over the classical laminated plate theory.

Recently, several exact solutions for composite material structures have been developed which indicate that Mindlin-type theories with five kinematic parameters do not adequately model the behavior of highly orthotropic composite structures. Therefore, a suitable higher-order plate theory is necessary to improve the accuracy of Mindlin-type plate theory.

The higher-order terms are needed in the power series expansions of the assumed displacement field to properly model the behavior of the laminates. Many different higher-order theories[23–28] have been proposed for the analysis of composite plates. A theory was given by Nelson and Lorch[23] for application to laminates, employing nine generalized coordinates in the kinematic assumptions. This higher-level theory is based on the assumed displacement forms:

$$\begin{aligned}\bar{u}_1 &= (u_x + z\varphi_y + z^2\xi_x)\\ \bar{u}_2 &= (u_y + z\varphi_y + z^2\xi_y)\\ \bar{u}_3 &= (w_x + z\varphi_z + z^2\xi_z)\end{aligned} \tag{2}$$

The higher-order theory extends classical theory to include transverse shear, transverse normal and quadratic displacement terms in the kinematic assumptions. In these higher-order shears deformation theories the conditions of zero transverse shear stresses on the top and bottom surfaces of the plate are not satisfied, and a shear correction to the transverse shear stiffness is required. Reddy[24] provided a new theory in which the displacement field chosen is of a special form. This requires the use of a displacement field in which the in-plane displacements are expanded as cubic functions of the thickness coordinate and the transverse deflection is constant through the plate thickness. This displacement field takes the form

$$\begin{aligned}\bar{u}_1 &= u_x + z\varphi_x + z^2\xi_x + z^3\phi_x\\ \bar{u}_2 &= u_y + z\varphi_y + z^2\xi_y + z^3\phi_y\\ \bar{u}_3 &= w_x\end{aligned} \tag{3}$$

The field satisfies the condition that the transverse shear stress vanishes on the top and bottom surface. ξ_x and ξ_y equal zero. ϕ_x and ϕ_y *are* functions of other variables. The theory has the same unknowns (five variables) and, moreover, for a non-linear variation of the transverse shear deformation through the thickness, there is no necessity to use shear correction coefficients in computing the shear stresses[25].

Lo et al.[26,27] extended the displacement form as follows:

$$
\begin{aligned}
\bar{u}_1 &= u_x + z\varphi_x + z^2\xi_x + z^3\phi_x \\
\bar{u}_2 &= u_y + z\varphi_y + z^2\xi_y + z^3\phi_y \\
\bar{u}_3 &= w_x + z\varphi_z + z^2\xi_z
\end{aligned} \tag{4}
$$

A critical review of plate theories by Bert[28] indicated that the theory of Lo *et al.*[29] gives an exact prediction of the non-linear bending stress distribution. Brunelle and Robertson[29] proposed a semi-experimental formulation for an arbitrarily initially stressed thick plate. Using these equations, the effect of bending stress on the buckling response was studied.

A series of studies[30–37] regarding homogeneous and composite plates was published by Chen and Doong. They derived the governing equations of a bimodular composite thick plate in a general state of variable initial stress by the average stress method and studied vibration[30] and buckling[31] responses of bimodular thick plates. Obviously, the buckling characteristics of bimodular material plates are different from those of homogeneous plates. The post buckling behavior of a simply supported rectangular bimodular thick plate subjected to a pure bending stress plus an extensional in-plane stress was studied by Chen and Doong[35–37]. The results are shown that bimodular properties and in-plane bending stress have significant effects on the post-buckled deflections of bimodular thick plates. At this work a deeply study by using higher-order shear deformation theory is performed to study buckling response of single- and two-layer cross-ply bimodular laminated plates. The aspect ratio, thickness ratio and bending stresses were shown to investigate effect of the buckling coefficient K_{cr}, for bimodular materials.

Moreover numerous analytical and numerical methods have been proposed for buckling and post-buckling analysis of different types of composites structures (example[38–40]).

At this work a deeply study by using higher-order shear deformation theory is performed to study buckling response of single- and two-layer cross-ply bimodular laminated plates. The aspect ratio, thickness ratio and bending stresses were shown to investigate effect of the buckling coefficient K_{cr}, for bimodular materials.

2. Modified Higher-Order Theory

Brunel and Robertson[29] derived the governing equations for initially stressed thick plates. They used incremental deformations and Hamilton's principle to obtain solutions. The results indicate that the transverse shear effects can decrease the stability of the plate and that initial bending stresses can cause a drastic reduction in the buckling load. The buckling coefficients depend on aspect ratio, thickness ratio and the ratio of bending to normal stresses. Brunel and Robertson's method was extended to bimodular plates. The governing equations of orthotropic materials may be used for bimodular materials, but Hooke's law, i.e. the stress-strain relation, must be of bimodular form. Based on the above explanations, Chen and Doong investigated the vibration[30] and buckling[31] of bimodular plates. Also, a bimodular composite material plate based on Mindlin plate theory was considered in those studies. More accurate analyses of bimodular composite plate problems, based on higher-order plate theory, are contained in a series of studies[30–39].

The governing equations are based on a higher-order theory of bi modular composite plates. For a cross-ply composite plate, the laminate stiffness's C_{16kl}, C_{26kl}, C_{36kl} and C_{45kl} will be equal to zero. The governing equations for orthotropic materials may be used for bimodular materials. The stress-strain relation must be of the bimodular form as follows:

$$
\begin{bmatrix} \bar{\sigma}_x \\ \bar{\sigma}_y \\ \bar{\sigma}_z \\ \bar{\sigma}_{yz} \\ \bar{\sigma}_{xz} \\ \bar{\sigma}_{xy} \end{bmatrix} = \begin{bmatrix} C_{11kl} & C_{12kl} & C_{13kl} & 0 & 0 & 0 \\ C_{12kl} & C_{22kl} & C_{23kl} & 0 & 0 & 0 \\ C_{13kl} & C_{23kl} & C_{33kl} & 0 & 0 & 0 \\ 0 & 0 & 0 & C_{44kl} & 0 & 0 \\ 0 & 0 & 0 & 0 & C_{5kl} & 0 \\ 0 & 0 & 0 & 0 & 0 & C_{66kl} \end{bmatrix} = \begin{bmatrix} \varepsilon_x \\ \varepsilon_y \\ \varepsilon_z \\ \varepsilon_{yz} \\ \varepsilon_{xz} \\ \varepsilon_{xy} \end{bmatrix} \tag{5}
$$

where C_{ijkl} are the stiffness coefficients of the stress-strain relation, the third subscript *(k)* refers to the sign of the strain ($k = t$ for tension and $k = c$ for compression) and the fourth subscript m denotes the layer number *(l= 1* to, n is the total number of layers). From the stress-strain relations, it can be seen that there are now 18 independent elastic stiffness coefficients for each orthotropic layer, a set of nine material variables for tension and another set of nine for compression.

We should consider a body in a state of non-uniform initial stress, which is in static equilibrium. Following the technique described by Brunelle and Robertson[29], the governing equations in rectangular Cartesian coordinates could be derived by using a perturbation technique. The governing equations are written as follows[29]:

$$\left(\sigma_{ij}\bar{u}_{s,j}\right)_{,i} + \bar{\sigma}_{i,j}(\delta_{s,j} + u_{s,j} + \bar{u}_{s,j})_{,i} + \bar{F}_s + \triangle F_s = \rho \ddot{\bar{u}}_s$$
$$\bar{P}_s + \triangle P_s = \left[\sigma_{ij}\bar{u}_{s,j} + \sigma_{ij}(\delta_{js} + u_{s,j} + \bar{u}_{s,j})\right]n_i \tag{6}$$

where $\bar{\sigma}_{ij}, \sigma_{ij}, \bar{F}_i$ and $\bar{P}_i$ are the initial stresses, perturbing stresses, body forces and applied surface tractions, respectively. It is assumed that initial displacement gradients are small and the equilibrium is static so that the products $\bar{\sigma}_{ij}u_{sj}$ and, $\rho\ddot{\bar{u}}_s$ can be neglected. For the large deflection plate theory, von Karman's assumptions are employed to investigate post-buckling behavior. Therefore, the perturbed displacement gradients are also small so that the terms $\bar{\sigma}_{ij}\bar{u}_{s,j}$ may be dropped except for $\bar{\sigma}_{i1}\bar{u}_{3,1}$, and $\bar{\sigma}_{i2}\bar{u}_{3,2}$. In order to give clarity to the integration procedure, it is useful to partially write out equation (6):

$$\frac{\partial(\sigma_{ij}\bar{u}_1/\partial x_j)}{\partial x_i} + \frac{\partial\bar{\sigma}_{i1}}{\partial x_i} + \bar{F}_1 + \triangle F_1 = 0$$
$$\frac{\partial(\sigma_{ij}\bar{u}_2/\delta x_j)}{\partial x_i} + \frac{\partial\bar{\sigma}_{i2}}{\partial x_i} + \bar{F}_2 + \triangle F_2 = 0 \tag{7}$$
$$\frac{\partial(\sigma_{ij}\bar{u}_3/\partial x_j)}{\partial x_i} + \frac{\partial\bar{\sigma}_{i3}}{\partial x_i} + (\bar{\sigma}_{i1}\bar{u}_{3,1})_{,i}(\bar{\sigma}_{i1}\bar{u}_{3,2}) + \bar{F}_3 + \triangle F_3 = 0$$

The non-linear stress-displacement relations of an orthotropic plate are as follows:

$$\bar{\sigma}_x = C_{11kl}\left(\bar{u}_{1,x} + \frac{1}{2}(\bar{u}_{3,x})^2\right) + C_{12kl}\left(\bar{u}_{2,y} + \frac{1}{2}(\bar{u}_{3,y})^2\right) + C_{13kl}\left(\bar{u}_{3,z} + \frac{1}{2}(\bar{u}_{3,z})^2\right)$$
$$\bar{\sigma}_x = C_{12kl}\left(\bar{u}_{1,x} + \frac{1}{2}(\bar{u}_{3,x})^2\right) + C_{22kl}\left(\bar{u}_{2,y} + \frac{1}{2}(\bar{u}_{3,y})^2\right) + C_{23kl}\left(\bar{u}_{3,z} + \frac{1}{2}(\bar{u}_{3,z})^2\right) \tag{8}$$
$$\bar{\sigma}_x = C_{13kl}\left(\bar{u}_{1,x} + \frac{1}{2}(\bar{u}_{3,x})^2\right) + C_{23kl}\left(\bar{u}_{2,y} + \frac{1}{2}(\bar{u}_{3,y})^2\right) + C_{33kl}\left(\bar{u}_{3,z} + \frac{1}{2}(\bar{u}_{3,z})^2\right)$$
$$\bar{\sigma}_{yz} = C_{44kl}\left(\bar{u}_{2,z} + \bar{u}_{3,y} + \bar{u}_{3,y} + \bar{u}_{3,z}\right)$$
$$\bar{\sigma}_{xz} = C_{55kl}\left(\bar{u}_{1,z} + \bar{u}_{3,x} + \bar{u}_{3,x} + \bar{u}_{3,z}\right)$$
$$\bar{\sigma}_{xz} = C_{66kl}\left(\bar{u}_{1,y} + \bar{u}_{2,x} + \bar{u}_{3,x} + \bar{u}_{3,y}\right)$$

For investigating the buckling problem, the von Karman assumptions ($\bar{\sigma}_{i1}\bar{u}_{3,1}$ and $\bar{\sigma}_{i2}\bar{u}_{3,2}$.) in equation (7) can be neglected and the governing equations become:

$$\partial(\sigma_{ij}\bar{u}_1/\partial x_j)\partial x_i + \partial\bar{\sigma}_{i1}/\partial x_i\bar{F}_1 + \triangle F_1 = 0$$
$$\partial(\sigma_{ij}\bar{u}_2/\partial x_j)\partial x_i + \partial\bar{\sigma}_{i2}/\partial x_i\bar{F}_2 + \triangle F_2 = 0 \tag{9}$$
$$\partial(\sigma_{ij}\bar{u}_3/\partial x_j)\partial x_i + \partial\bar{\sigma}_{i3}/\partial x_i\bar{F}_3 + \triangle F_3 = 0$$
$$\bar{P}_s + \triangle P_s = (\sigma_{ij}\bar{u}_{s,j}/\bar{u}_{i,j,j})n_i$$

The linear stress-displacement relations of an orthotropic bimodular plate are given by:

$$\bar{\sigma}_x = C_{11kl}\bar{u}_{1,x} + C_{12kl}\bar{u}_{2,y} + C_{13kl}\bar{u}_{3,z}$$
$$\bar{\sigma}_y = C_{12kl}\bar{u}_{1,x} + C_{22kl}\bar{u}_{2,y} + C_{23kl}\bar{u}_{3,z}$$
$$\bar{\sigma}_x = C_{13kl}\bar{u}_{1,x} + C_{22kl}\bar{u}_{2,y} + C_{33kl}\bar{u}_{3,z} \tag{10}$$
$$\bar{\sigma}_{yz} = C_{44kl}(\bar{u}_{2,z} + \bar{u}_{3,y})$$
$$\bar{\sigma}_{xz} = C_{55kl}(\bar{u}_{1,z} + \bar{u}_{3,x})$$
$$\bar{\sigma}_{xz} = C_{66kl}(\bar{u}_{1,y} + \bar{u}_{2,x})$$

At this work the governing equations of a plate are derived in a general state of non-uniform initial stress based on a new higher-order plate theory with seven kinematic variables. The displacements are the same of Lo et al.[22,23] but the transverse shear stresses, τ_{xz} and τ_{yz}, are vanished on the top and bottom surfaces of the plate. These conditions are equivalent to the requirement that the corresponding strains are zero on these surfaces for orthotropic plates or plates laminated of orthotropic layers, i.e., $\gamma_{zx}(x, y, \pm h)=0$ and $\gamma_{yz}(x, y, \pm h)=0$ (Figure 1). The displacements then become:

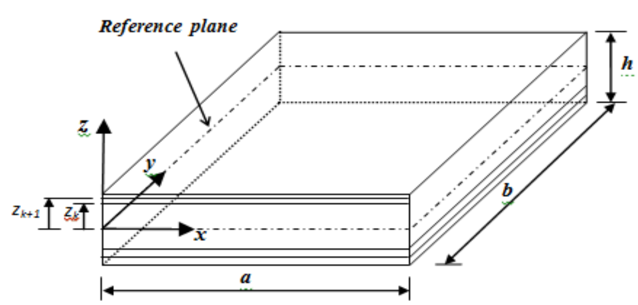

Figure 1. Geometry and coordinate system of bimodular laminated plate.

$$
\begin{aligned}
u_1 &= u_x + \left[\varphi_x - \frac{1}{2} z\varphi_{z,x} - \frac{4}{3}\left(\frac{z}{h}\right)^2 \left(w_{,x} + \varphi_x + \frac{h^2}{4}\xi_{z,x}\right)\right] \\
u_2 &= u_y + \left[\varphi_y - \frac{1}{2} z\varphi_{z,y} - \frac{4}{3}\left(\frac{z}{h}\right)^2 \left(w_{,y} + \varphi_y + \frac{h^2}{4}\xi_{z,y}\right)\right]
\end{aligned} \quad (11)
$$

Following similar procedure to Brunelle's method[26] and Doong's procedure[34], a simply supported rectangular bimodular plate in a state of bending stress plus a compressive stress could be studied. The state of initial stress is

$$\sigma_{11} = \sigma_n + 2z\sigma_m/h \quad (12)$$

σ_n and σ_m are taken constants and all other initial stresses are assumed to be zero. It is comprised of a tensile (compressive) stress σ_n plus a bending stress σ_m. The only non-zero force and moment resultants are as follows:

$$
\begin{aligned}
&N_{xx} = \int \sigma_{11} dz = h\sigma_{n'} && M_{xx} = \int \sigma_{11} z dz = h^2\sigma_m/6 \\
&N^*_{xx} = \int \sigma_{11} z^2 dz = h^3\sigma_n/12 && P_{xx} = \int \sigma_{11} z^3 dz = h^4\sigma_m/40 \\
&P^*_{xx} = \int \sigma_{11} z^4 dz = h^5\sigma_n/80 && R_{xx} = \int \sigma_{11} z^5 dz = h^6\sigma_m/40 \\
&R^*_{xx} = \int \sigma_{11} z^6 dz = h^7\sigma_n/448
\end{aligned} \quad (13)
$$

All above integrals are through the thickness of the plate from *-h/2* to *h/2*. Lateral loads and body forces are assumed to be zero. Based on the above explanations, the governing equations and boundary conditions can be derived.

$$
\begin{aligned}
&Q_{1,x} + Q_{2,y} + R_{1,x} = 0 \qquad Q_{2,x} + Q_{3,y} + R_{9,x} = 0 \\
&Q_{4,x} + Q_{5,y} + R_{30,x} + \left(\frac{4}{3}h^2\right)(Q_{18} + 2Q_{19,xy} + Q_{20} - 3Q_{15,x} - 3Q_{15,y} + R_{4,xx} + R_{12,xy}) = 0 \\
&Q_{6,x} + Q_{7,y} - Q_4 + R_{2,x} - \left(\frac{4}{3}h^2\right)(Q_{18} + Q_{19,y} - 3Q_{15} + R_{4,x} = 0 \\
&Q_{7,x} + Q_{8,y} - Q_5 + R_{10,x} - \left(\frac{4}{3}h^2\right)(Q_{19} + Q_{20,y} - 3Q_{16} + R_{12,x} = 0 \\
&-Q_{11} + R_{3,1} + \frac{1}{2}(Q_{12,xx} + 2Q_{13,xy} + Q_{14,yy} + R_{3,xx} + R_{11,xy}) = 0 \\
&-2Q_{17} + R_{3,2} + \frac{1}{2}(Q_{18,xx} + 2Q_{19,xy} + Q_{20,yy} + R_{4,xx} + R_{12,xy}) = 0
\end{aligned} \quad (14)
$$

For the simply supported plate, the boundary conditions along the x = constant edges are taken as follows:

$$
\begin{aligned}
&u_y = 0;\ \varphi_y = 0;\ w = 0\ \ \varphi_z = 0;\ \xi_z = 0 \\
&\overline{N}_{xx} + \triangle N_{xx} = Q_1 + R_1;\ \overline{M}^*_{xx} + \triangle M^*_{xx} = -\frac{1}{2}(Q_{12} + R_3) \\
&\overline{P}_{xx} + \triangle P_{xx} = -\frac{4}{3h^2}(Q_{18} + R_4);\overline{T}_{xx} + \triangle T_{xx} = -\frac{1}{2}(Q_{18} + R_4) \\
&\overline{M}_{xx} + \triangle M_{xx} = (Q_6 + R_2) - \frac{4}{3h^2}(Q_{18} + R_4)
\end{aligned} \quad (15)
$$

Displacements of the following form satisfy the

$$
\begin{aligned}
&u_x = 0;\ \varphi_x = 0;\ w = 0\ \ \varphi_z = 0;\ \xi_z = 0 \\
&\overline{N}_{yy} + \triangle N_{yy} = Q_3;\ \overline{M}^*_{yy} + \triangle M^*_{yy} = -\frac{1}{2}Q_{14} \\
&\overline{P}_{yy} + \triangle P_{yy} = -\frac{4}{3h^2}Q_{20};;\overline{T}_{yy} + \triangle T_{yy} = -\frac{1}{3}Q_{20} \\
&\overline{M}_{yy} + \triangle M_{yy} = Q_8 - \frac{4}{3h^2}Q_{20}
\end{aligned} \quad (16a)
$$

And

$$\left(\overline{N}_{ii},\overline{P}_{ii},\overline{M}_{ii},\overline{M}^{*}_{ii},\overline{T}_{ii},\right)=\int \overline{P}_i\left[1,-\frac{4}{3h^2}z^3,z-\frac{4}{3h^2}z^3-\frac{1}{2}z^2,\frac{1}{3}z^2\right]dz$$
$$\left(\triangle N_{ii},\triangle P_{ii},\triangle\overline{M}_{ii},\triangle M^{*}_{ii},\triangle T_{ii}\right)=\int \triangle P_i\left[1,-\frac{4}{3h^2}z^3,z-\frac{4}{3h^2}z^3,-\frac{1}{2}z^2,\frac{1}{3}z^2\right]dz(i=x,y) \quad (16b)$$

boundary conditions

$u_x=\Sigma\Sigma hU_{mn}\cos(m\pi x/a)\sin(n\pi y/b)$
$u_y=\Sigma\Sigma hV_{mn}\sin(m\pi x/a)\cos(n\pi y/b)$
$\omega=\Sigma\Sigma hW_{mn}\sin(m\pi x/a)\sin(n\pi y/b)$
$\varphi_x=\Sigma\Sigma\psi_{xmn}\cos(m\pi x/a)\sin(n\pi y/b)$
$\varphi_y=\Sigma\Sigma\psi_{ymn}\sin(m\pi x/a)\cos(n\pi y/b)$
$\varphi_z=\Sigma\Sigma\psi_{zmn}\sin(m\pi x/a)\sin(n\pi y/b)$
$\xi_z=\Sigma\Sigma(\zeta_{zmn}/h)_{xmn}\sin(m\pi x/a)\sin(n\pi y/b)$ (17)

Substituting the displacement field of equations (17) into equations (14) yields:

$([C]\lambda[G])\{\Delta\}=\{0\}$

$\{\Delta\}=\{U_{mn}, V_{mn}, W_{mn}, \psi_{xmn}, \psi_{ymn}, \psi_{zmn},\zeta_{zmn}\}^T$ (18)

To determine the position of the neutral surface, the strains in the x, y directions must be equal to zero :

The non-dimensional neutral surface locations z_{nx}, z_{ny}

$$\varepsilon_x=U_{x,x}+z\varphi_{x,x}+\frac{1}{2}z^2\varphi_{z,xx}-\frac{4}{3h^2}\left(\omega_{,xx}+\varphi_{x,x}+\frac{h^2}{4}\xi_{z,xx}\right)=0$$
$$or\ z_{nx}/h=\left[\frac{1}{2}\alpha z_{nx}^2\psi_{xmn}+\frac{4}{3}z_{nx}^3\left(\alpha W_{mn}+\psi_{xmn}+\frac{1}{4}\xi_{xmn}\right)-U_{mn}\right]/\psi_{xmn}$$
$$And\ \varepsilon_y=U_{x,x}+z\varphi_{y,y}+\frac{1}{2}z^2\varphi_{z,yy}-\frac{4}{3h^2}\left(\omega_{,yy}+\varphi_{y,y}+\frac{h^2}{4}\xi_{z,xx}\right)=0 \quad (19)$$
$$z_{ny}/h=\left[\frac{1}{2}\beta z_{ny}^2\psi_{xmn}+\frac{4}{3}z_{ny}^3\left(\alpha W_{mn}+\psi_{xmn}+\frac{1}{4}\beta\xi_{xmn}-V\right)\right]/\psi_{ymn}$$

are defined as

$$z_{nx}=z_{nx}/h=\left[\frac{1}{2}\alpha z_{nx}^2\psi_{xmn}+\frac{4}{3}z_{nx}^3\left(\alpha W_{mn}+\psi_{xmn}+\frac{1}{4}\xi_{xmn}\right)\right.$$
$$z_{ny}=z_{ny}/h=\left[\frac{1}{2}\beta z_{ny}^2\psi_{xmn}+\frac{4}{3}z_{ny}^3\left(\alpha W_{mn}+\psi_{ymn}+\frac{1}{4}\xi_{ymn}\right)\right. \quad (20)$$
$$K_5=0$$

3. Numerical Results and Discussion

3.1 Buckling of Bimodular Rectangular Plates

There are many anisotropic variables which have effects on the buckling load. For a single cross-ply layer, non-dimensional buckling coefficients are shown in Figures 1-6. In the computations, $E^c = 1.0$, $v^c = 0.2$, $E^t/E^c = 0.2$-2.0 and v^t is given by the relation $v^t = v^c E^t/E^c$. The shear moduli G^t and G^c in the compressive and tensile regions respectively are $G^c = E^c/2(1+v^c)$, G^t.

Variation of the buckling coefficient K_{cr}, for various E^t/E^c ratios is shown in Figure 1, where a/h, a/b, and S are equal to 10, 1 and 0, respectively. It can be seen that the buckling coefficient has the greatest value when E^t/E^c is equal to 1.0. The neutral planes of higher-order plate theory results are further away from the middle plane than those of Mindlin plate (first-order) theory results. This figure also shows that the buckling coefficients of the higher-order plate theory are lower than those of the first-order theory.

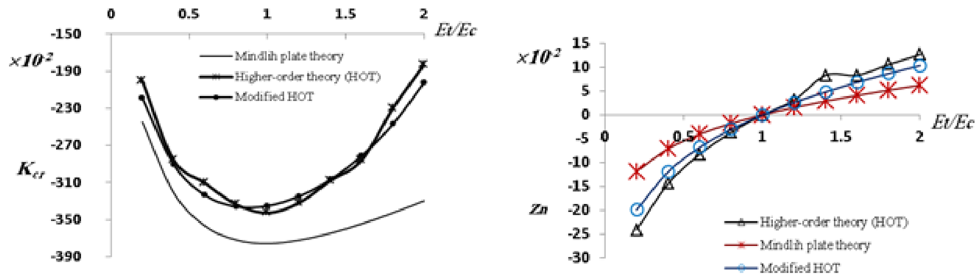

Figure 2. Buckling coefficients for various E^t/E^c values ($a/b = 1$, $a/h = 10$, $S=\sigma_m/\sigma_n=0$, $\nu^c=0.2$).

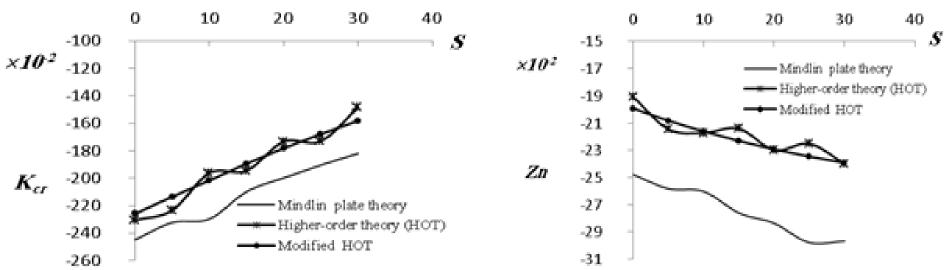

Figure 3. Buckling coefficients for various values of the bending stress to normal stress ratio ($E^t/E^c = 0.2$, $a/b = 1$, $a/h = 1$, $\nu^c = 0.2$).

The influence of the bending stress on the buckling load is shown in Figures 2 and 3. The effects on the buckling coefficients are shown for a value of $E^t/E^c<1.0$. The reverse effect can be observed for a bimodular plate with. The main reason for the difference between $E^t/E^c>1.0$ and $E^t/E^c<1.0$ buckling coefficients in bimodular plates is due to the change in position of the neutral plane Z_n. The buckling coefficients are larger where the neutral plane is closer to the mid-plane of plate.

Effects of the thickness ratio a/h on the buckling

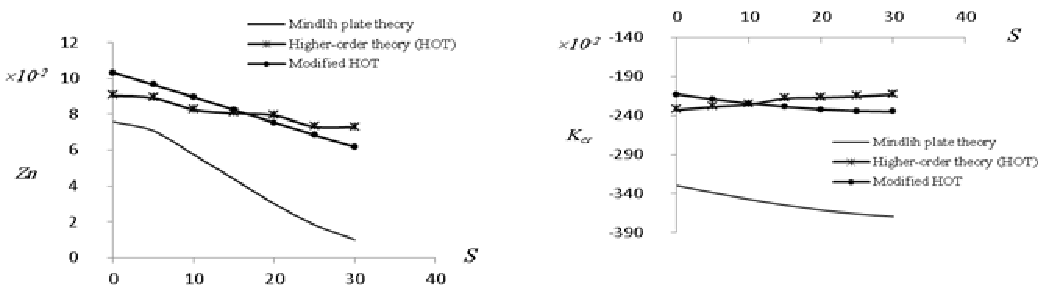

Figure 4. Buckling coefficients for various values of the bending stress to normal stress ratio ($E^t/E^c=2$, $a/b = 1$, $a/h=10$, $\nu^c=0.2$).

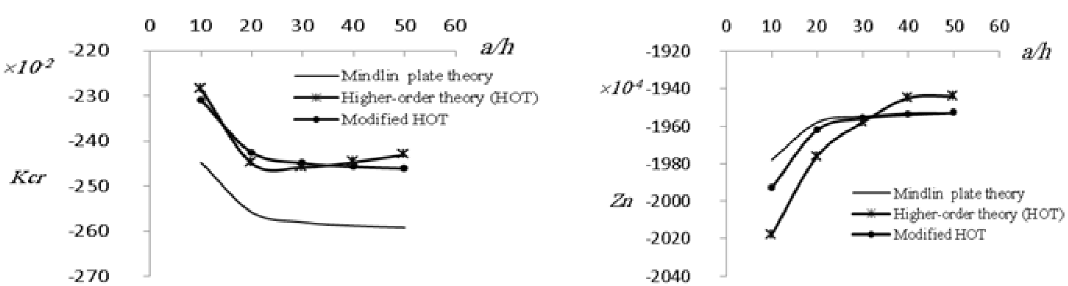

Figure 5. Effect of thickness ratio a/h on buckling coefficients ($E^t/E^c=0.2$, $a/b=1$, $S=\sigma_m/\sigma_n=0$, $\nu^c=0.2$).

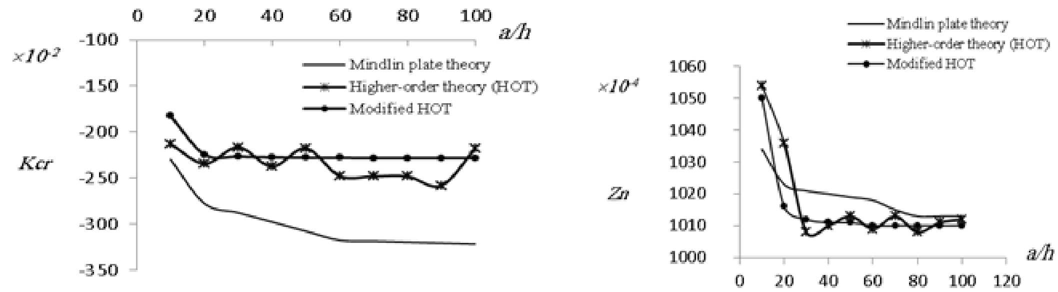

Figure 6. Effect of thickness ratio a/h on buckling coefficients ($E^t/E^c=2$, $a/b=1$, $S=\sigma_m/\sigma_n=0$, $\upsilon^c=0.2$).

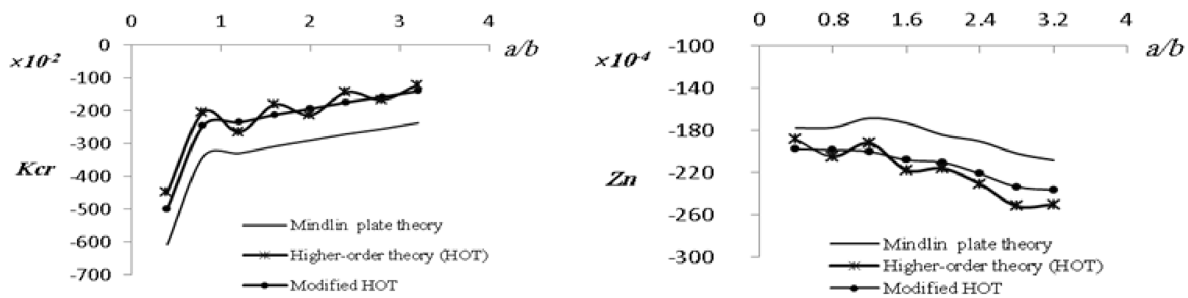

Figure 7. Effect of aspect ratio a/b on buckling coefficients ($E^t/E^c=0.2$, $a/h=10$, $S=\sigma_m/\sigma_n=0$, $\upsilon^c=0.2$).

coefficients are shown in Figures 4 and 5. The higher-order shear deformation variables have little effect on the neutral surface location Z_n for thin plates. The meaningful influence of higher-order shear deformation variables on Z_n can be observed as the thickness increases and the buckling coefficients decrease with decreasing thickness ratio.

The effect of aspect ratio on buckling load is shown in Figures 6 and 7 where *a/h*, E^t/E^c and *S* are equal to 10, 0.2-2.0 and 0, respectively. It is observed that the larger the aspect ratio *a/b*, the lower the buckling coefficient, and the further the neutral plane location is from the middle of plate. Also, higher order shear deformation parameters have meaningful effects on Z_n for high aspect ratio bimodular plates.

The results of the modified higher order plate theory are compared with those of the higher-order plate theory in Figures 1 to 7. The effects of modulus ratio, laminate thickness and bending stress on the buckling loads are examined. Using the new modified plate theory, the computed buckling coefficients agree well with those of the higher-order plate theory, but the displacement field of the new modified plate theory satisfies the stress-free boundary conditions. The benefit of significant simplification compared with the higher-order theory order increases its utility in analyzing the bending of plates. Buckling analysis using the finite strip method was developed for bimodular laminated plates by Lee[38]. Compared to analytical solutions, excellent agreement was observed for thick composite plates (Figures 8 to

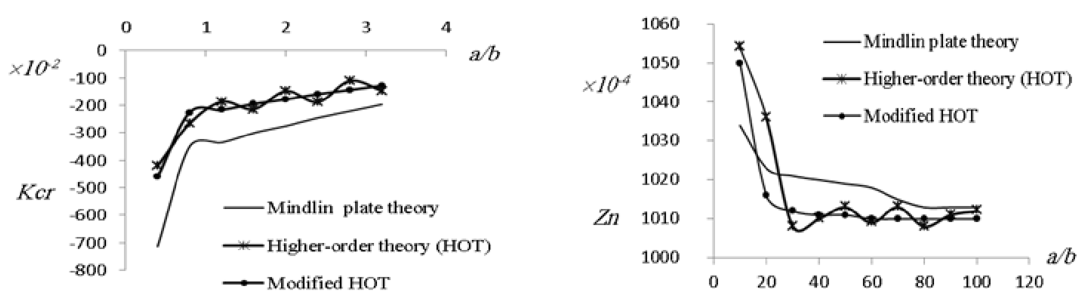

Figure 8. Effect of aspect ratio a/b on buckling coefficients ($E^t/E^c=2$, $a/h=10$, $S=\sigma_m/\sigma_n=0$, $\upsilon^c=0.2$).

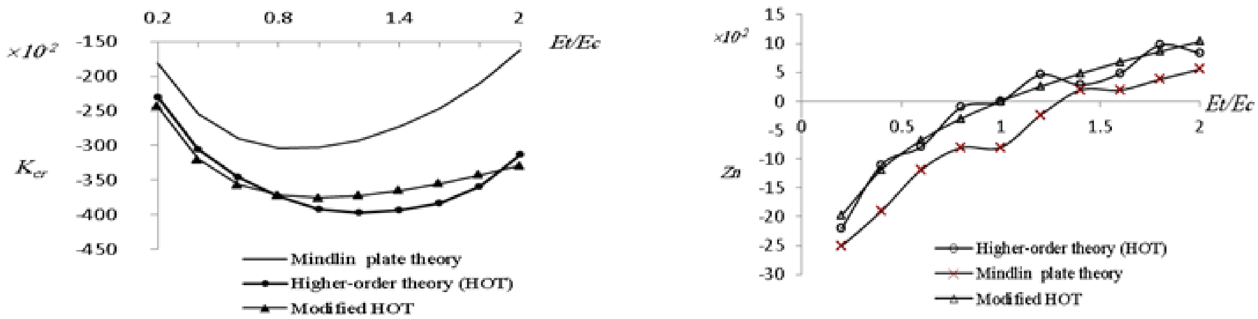

Figure 9. Influence of E^t/E^c on buckling coefficients ($a/b=1$, $S=\sigma_m/\sigma_n=0$, $\nu^c=0.2$, $a/h=10$).

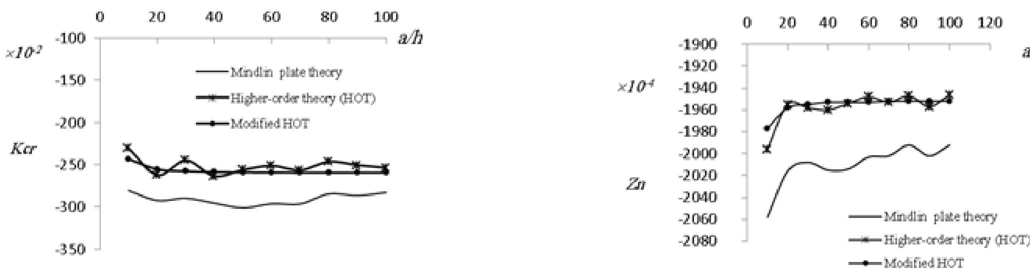

Figure 10. Effect of thickness ratio a/h on buckling coefficients ($E^t/E^c=0.2$, $a/b=1$, $S=\sigma_m/\sigma_n=0$, $\nu^c=0.2$).

10). It is also observed that the higher-order theory yields more accurate results than the first-order theory.

3.2 Buckling of Bimodular Laminated Plates

For a two-layer cross-ply laminated, the influences of aspect ratio on buckling load and neutral plane location are given in Figure 11. The buckling coefficient decreases with increasing aspect ratio and the neutral surface is further away from the middle plane.

Variation of buckling coefficients versus E_2^t / E_2^c and thickness ratio *a/h* are shown in Figures 12 to 14. The modified seven-variable plate theory and the higher-order plate result closely the same buckling coefficients. As the thickness ratio increases, the differences are larger between the new modified plate theory and the higher-order theory larger.

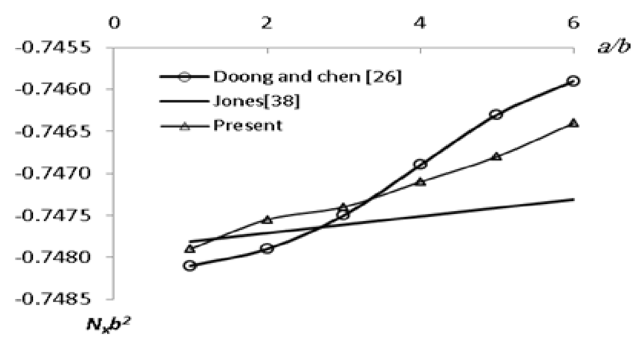

Figure 11. Buckling loads of two-layer cross-ply laminated plates ($E_1/E_2=40, G_{12}/E_2=0.5, \upsilon_{12}=0.25$).

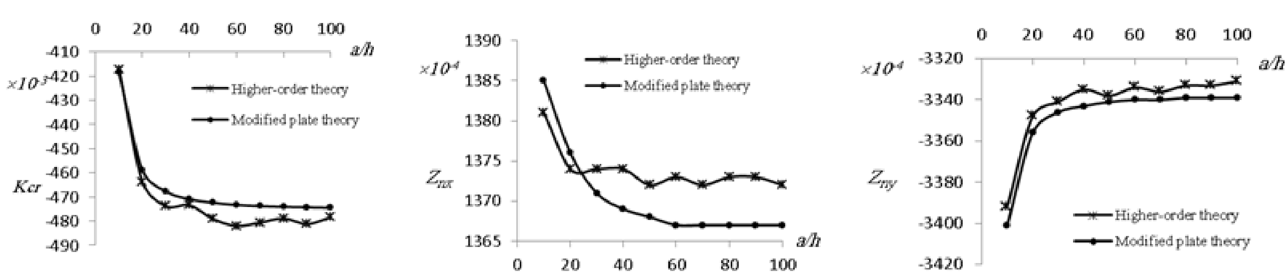

Figure 12. Effect of the thickness ratio a/h on buckling coefficient for two-layer cross-ply laminated plate ($a/b=1$, $S=0$, $E_2^t / E_2^c=0.2$).

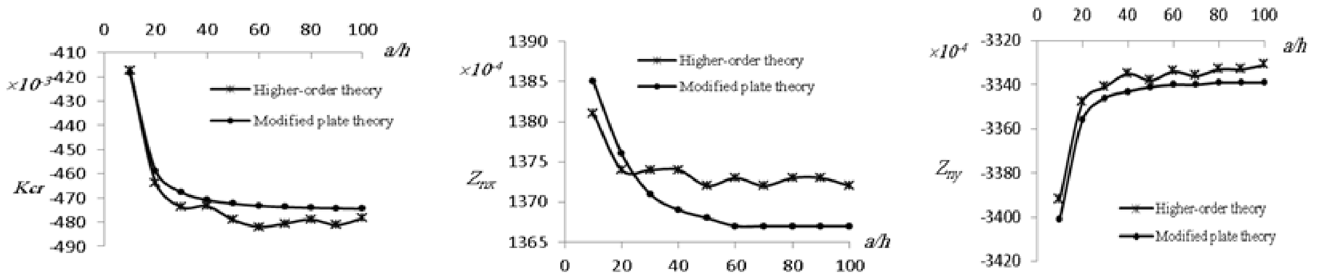

Figure 13. Effect of the thickness ratio a/h on buckling coefficient for two-layer cross-ply laminated plate (*a/b=1, S=0,* E_2^t / E_2^c *=2.0*).

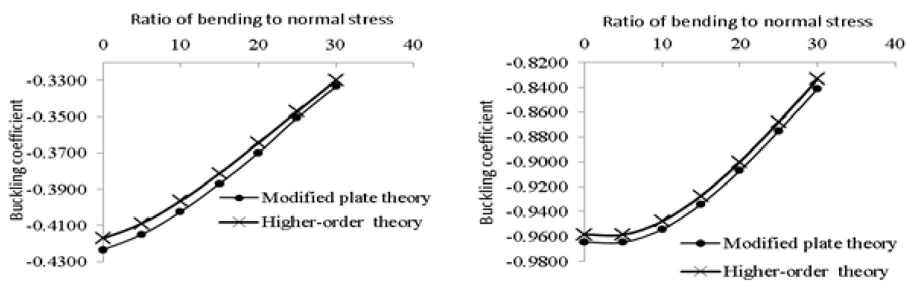

$E_2^t / E_2^c = 0.2$ $E_2^t / E_2^c = 2$

Figure 14. Effect of the ratio of bending stress to normal stress on buckling coefficient for two-layer cross ply laminated plate (*a/b=1, a/h=10*).

4. Conclusion

The principal results presented at this work demonstrate the following:

- The previously obtained eleven-variable higher order theory result is so complex that its utility is questionable. The present seven-variable modified plate theory gives nearly the same results as the previous solution.
- A new displacement field is proposed in the present work to satisfy boundary conditions.
- The parametric study is carried out to investigate the effect of aspect and thickness ratios, lay-up on geometrically linear and nonlinear buckling response of bimodular cross-ply composite laminates
- The buckling load is significantly affected by which others did not mention.

5. References

1. Khan AH, Patel BP. Nonlinear forced vibration response of bimodular laminated composite plates. Composite Structures. 2014; 108:524–37.
2. He XT, Chen Q, Sun JY, Zheng ZL, Chen SL. Application of the Kirchhoff hypothesis to bending thin plates with different moduli in tension and compression. Journal of Mechanics of Materials and Structures. 2010; 5:755–69.
3. Doong JL, Chen LW. Buckling of bimodular composite plates. Buckling and Post-buckling of Composite Plates. Netherlands: Springer; 1995. p. 227–59.
4. Timoshenko SP. Strength of Materials Part 2:Advanced Theory and Problems. 2nd ed. Princeton:Van Nostrand; 1941.
5. Ambartsumyan SA, Khachaturian AA. Basic equations in the theory of elasticity of materials with different stiffness in tension and compression. Mechanics of Solids. 1966; 1:29–34.
6. Shapiro GS. Deformation of bodies with different tensile and compressive strengths. Mechanics of Solids. 1966; 1:85–6.
7. Kamiya N. A circular cylindrical shell wi.th different elastic moduli in tension and compression. Bulletin of the Japanese Society of Mechanical Engineers. 1975; 18:1075–81.
8. Kamiya N. Large deflection of a different modulus circular plate. Trans SME Journal of Engineering Materials and Technology. 1975; 97:52–6.
9. Kamiya N. An energy method applied to large elastic deflection of a thin plate of bimodulus material. Journal of Structural Mechanics. 1975; 97:317–29.
10. Sun JY, Zhu HQ, Qin SH, Yang DL, He XT. A review on the research of mechanical problems with different moduli in tension and compression. Journal of Mechanical Science and Technology. 2010; 24(9):1845–54.

11. Bert CW. Classical Analyses of Laminated Bimodulus Composite-Material Plates (No. OU-AMNE-79-10A). Oklahoma University, Norman School of Aerospace Mechanical and Nuclear Engineering; 1979.
12. Bert CW, Reddy JN, Chao WC, Reddy VS. Vibration of thick rectangular plates of bimodulus composite materials. Journal of Applied Mechanics. 1981; 48:371–6.
13. Bert CW, Kumar M. Vibration of cylindrical shells of bimodulus composite materials. Journal of Sound and Vibration. 1982; 81:107–21.
14. Reddy JN, Chao WC. Finite element analysis of laminated bimodulus plates. Computers and Structures. 1980; 12:245–51.
15. Bert CW, Reddy JN, Reddy VS, Chao WC. Bending of thick rectangular plates laminated of bimodulus composite materials. AIAA Journal. 1981; 19:1342–9.
16. Jones RM. Buckling of cylindrical shells with different moduli in tension and compression. AlAA Journal. 1971; 9:53–61.
17. Jones RM. Buckling of stiffened multi1ayered circular cylindrical shells with different orthotropic moduli in tension and compression. AIAA Journal. 1971; 9:917–23.
18. Bert CW, Reddy JN. Vibration and buckling of thick cylindrical shells of bimodulus composite materials. Advances in Aerospace Structures and Materials. 1981; 109–14.
19. Hajmohammad MH, Salari M, Hashemi SA, Esfe MH. Optimization of Stacking Sequence of Composite Laminates for Optimizing Buckling Load by Neural Network and Genetic Algorithm. Indian Journal of Science and Technology. 2013; 6(8):5070–7.
20. Hwu C. Anisotropic elastic plates. Springer Science & Business Media; 2010.
21. Reissner E. The effects of transverse shear deformation on the bending of elastic plates. Journal of Applied Mechanics. 1945; 12:69–77.
22. Mindlin RD. Influence of rotatory inertia and shear on flexural motions of isotropic elastic plates. Journal of Applied Mechanics. 1951; 18:31–8.
23. Nelson RB, Lorch DR. A refined theory for laminated orthotropic plates. Journal of Applied Mechanics. 1974; 41:177–83.
24. Reddy JN. A simple higher-order theory for laminated composite plates. Journal of Applied Mechanics. 1984; 51:745–52.
25. Pajand MR, Shahabian F, Tavakoli FH. Delamination detection in buckling laminated composite plates. Proceedings of the ICE - Engineering and Computational Mechanics; 2014; 167:67–81.
26. Lo KH, Christensen HM, Wu EM. A higher-order theory of plate deformation. Part I. homogeneous plates. Journal of Applied Mechanics. 1977; 44:633–8.
27. Lo KH, Christensen HM, Wu EM. A higher-order theory of plate deformation, Part II: laminated plates. Journal of Applied Mechanics. 1977; 44:669–76.
28. Bert CW. A critical evaluation of new plate theories applied to laminated composites. Composite Structures. 1984; 2:329–47.
29. Brunelle EJ, Robertson SR. Initially stressed Mindlin plates. AIAA Journal. 1974; 12:1036–45.
30. Doong JL, Chen LW. Vibration of a bimodulus thick plate. Journal of Vibration, Acoustics, Stress and Reliability in Design. 1985; 107:92–7.
31. Doong JL, Chen LW. Buckling of a bimodulus composite thick plate. Proceedings of ASME, Failure Prevention and Reliability Conference; 1983. p. 11–4.
32. Iung CP, Doong JL. Bending of a bimodulus laminated plate based on a higher-order shear deformation theory. Composite Structures. 1988; 10:121–44.
33. Doong JL, Fung CP. Vibration and buckling of bimodulus laminated plates according to a higher-order plate theory. Journal of Sound and Vibration. 1988; 125:325–39.
34. Doong JL, Lee C, Fung CP. Vibration and stability of laminated plates based on a modified plate theory. Journal of Sound and Vibration. 1991; 151:193–201.
35. Chen LW, Doong JL. Post-buckling behavior of a thick plate. AIAA Journal. 1983; 21:1157–61.
36. Doong JL, Chen LW. Post-buckling behavior of a bimodulus thick plate. Journal of the Chinese Society of Mechanical Engineers. 1985; 6:137–44.
37. Doong JL. Vibration and stability of an initially stressed thick plate according to a higher-order deformation theory. Journal of Sound and Vibration. 1987; 113:425–40.
38. Kumar JS, Raju TD, Reddy KVK. Vibration analysis of composite laminated plates using higher-order shear deformation theory with zig-zag function. Indian Journal of Science and Technology. 2011; 4(8):960–6.
39. Yi GS. Anisotropic Constitutive Model for Predictive Analysis of Composite Laminates. Indian Journal of Science and Technology. 2015; 8(S1):189–93.
40. Farahani H, Barati F, Batmani H. Vibration Analysis of Composite Horizontal Cylindrical Tank with Different Layering Using the Finite Element Method. Indian Journal of Science and Technology. 2015; 8(S7):213–9.